EFFICIENT SORGHUM AND MAIZE TRANSFORMATION USING A TERNARY VECTOR SYSTEM COMBINED WITH MORPHOGENIC REGULATORS

Juan B. Fontanet-Manzaneque[1††], Jari Haeghebaert[2,3], Stijn Aesaert[2,3], Griet Coussens[2,3], Laurens Pauwels[2,3, †,*] and Ana I. Caño-Delgado[1, *]

[1]Department of Molecular Genetics, Centre for Research in Agricultural Genomics (CRAG) CSIC-IRTA-UAB-UB, Campus UAB (Cerdanyola del Vallès), 08193 Barcelona, Spain.

[2]Ghent University, Department of Plant Biotechnology and Bioinformatics, 9052 Ghent, Belgium.

[3]VIB-UGent Center for Plant Systems Biology, 9052 Ghent, Belgium.

[†]Current address: Department of Biotechnology, Faculty of Bioscience Engineering, Ghent University, Proeftuinstraat 86, 9000 Ghent, Belgium

[††] Current address: [3]VIB-UGent Center for Plant Systems Biology, 9052 Ghent, Belgium.

*Corresponding authors: Ana I. Caño-Delgado, E-mail: ana.cano@cragenomica.es and Laurens Pauwels laurens.pauwels@ugent.be

(I) SUMMARY

Sorghum bicolor (sorghum) is a vital C4 monocotyledon crop cultivated in arid regions worldwide, valued for its significance in both human and animal nutrition. Despite its agricultural prominence, sorghum research has been hindered by low transformation frequency. In this study we examined sorghum transformation using the pVS1-VIR2 ternary vector system for *Agrobacterium*, combined with the morphogenic genes *BABY BOOM* and *WUSCHEL2* and selection using G418. We optimized *Agrobacterium*-mediated infection, targeting key parameters such as bacterial optical density, co-cultivation time, and temperature. Additionally, an excision-based transformation system enabled us to generate transgenic plants free of morphogenic regulators. The method yielded remarkable transformation frequencies, reaching up to 164.8% based on total isolated plantlets. The same combination of ternary vector, morphogenic genes and geneticin-based selection also resulted in a marked increase in transformation efficiency of the *Zea mays* (maize) inbred line B104. The potential for genomic editing using this approach positions it as a valuable tool for the development of sorghum and maize varieties that comply with evolving European regulations.

Our work marks a significant stride in sorghum biotechnology and holds promise for addressing global food security challenges in a changing climate.

(II) SIGNIFICANCE STATEMENT

This study achieved unprecedented transformation frequencies in *Sorghum bicolor* using the pVS1-VIR2 ternary vector system combined with *BABY BOOM* and *WUSCHEL2* morphogenic genes. These advancements promise to enhance sorghum and maize breeding, addressing global food security in a changing climate.

KEY WORDS

Sorghum bicolor

Transformation

Morphogenic regulators

Ternary vector

BABY BOOM

WUSCHEL2

Zea mays

(III) INTRODUCTION

Sorghum bicolor (sorghum) is a C4 monocotyledon crop widely grown in Africa and South Asia in arid and semi-arid regions for its use as a staple food and fodder. In addition, it is grown in countries such as the United States, Mexico, Brazil and Australia, mainly as animal feed. Together this makes sorghum the 5th most important cereal crop in terms of production (Mullet et al.,2002; FAOSTAT, 2022).

Several studies rely on natural variation to find alleles to improve desirable traits for sorghum breeding, including better quality grains or ability to tolerate drought stress (Ortiz et al., 2021; Xie et al., 2022). Despite relatively well-understood and conserved molecular pathways, there has been limited progress in using genetic engineering to accelerate the development of sorghum varieties that are better suited to the current climate crisis. Sorghum is still considered a crop recalcitrant to genetic transformation given its low regeneration and

accumulation of phenolics during tissue culture (Visarada and Kishore, 2015; Miller et al., 2023).

Genetic transformation of sorghum is traditionally done with microprojectile bombardment using immature embryos as explants. Initially, only 2 out of 600 embryos yielded transgenics, resulting in an unworkable 0.3% transformation efficiency (Casas et al., 1993). Since then, significant progress has been made in sorghum particle bombardment-mediated transformation, with reports up to 20.7% (Liu and Godwin, 2012).

Agrobacterium tumefaciens (*Agrobacterium*)-mediated transformation is however a preferred technology as particle bombardment can lead to structural genome rearrangements (Yue *et al*., 2022). In 2000, the use of *Agrobacterium* to genetically transform sorghum immature embryos was first reported, obtaining very variable transformation efficiencies from 0.17 to 10.1 % (Zhao et al., 2000). The implementation of the use of morphogenic regulators was a breakthrough in immature embryo-based transformation in monocots. *Agrobacterium*-mediated transformation of maize *BABY BOOM (Bbm)* and *WUSCHEL2 (Wus2)* in maize inbred lines led to high transformation frequencies and genotype-flexibility of regeneration (Lowe et al. 2016). The morphogenic genes were used together with a novel ternary vector system. The latter allowed equipping *Agrobacterium* with extra virulence genes, improving the transfer DNA (T-DNA) delivery (Anand et al., 2018; Zhang et al., 2019; Aliu et al., 2024). The combination of these two new techniques has led to an immature embryo-based and genotype-flexible sorghum transformation system, having the highest transformation frequency reported up to now of 69.7 % (Che et al. 2022).

Nonetheless, expressing *Bbm* and *Wus2* has a limitation. These morphogenic regulators have the desirable effect of boosting somatic embryo formation but also have undesirable pleiotropic effects when constitutively expressed in T0 plants. To avoid this limitation, several strategies were developed such as a Cre/Lox-mediated excision system and a method designated as “altruistic transformation”. The excision system is based on three expression cassettes containing *Bbm*, *Wus2* and a *CRE* recombinase, flanked by LoxP recombination target sites. *CRE* is driven by an inducible promoter, therefore resulting in an inducible system to excise the morphogenic expression cassettes (Gordon-Kamm et al., 2019). The “altruistic transformation” is based on a co-transformation system in which two *Agrobacterium* strains are used for transformation. The first strain will carry the “altruistic T-DNA” with morphogenic regulator expression cassette but lacking a selectable marker. The second will contain the gene of interest and the presence of a selectable marker. The rationale is that morphogenic

regulator proteins can move to neighboring cells, enhancing the somatic embryogenesis and non-morphogenic regulator containing cells will have the ability to be efficiently transformed through somatic embryo formation (Hoerster et al., 2020; Aregawi et al., 2022; Kang et al., 2023). In both systems regenerated plants carrying the gene of interest are generated yet lacking the integration of morphogenic regulators.

In this study, we evaluated morphogene-assisted transformation for sorghum using the publicly available pVS1-VIR2 ternary vector system combined with a newly designed and compatible binary destination vector. We improved conditions for *Agrobacterium* co-cultivation and the pressure of the selectable agent in order to obtain significantly higher sorghum transformation efficiencies than those previously reported.

(IV) RESULTS

Optimizing *Agrobacterium* co-cultivation conditions.

In this study, we conducted an optimization of *Agrobacterium* infection by using the *Agrobacterium* strain EHA105 recA$^-$ containing the ternary helper vector pVS1-VIR2 (Rodrigues, et al., 2021; Zhang et al., 2019) . We evaluated adjustments of several factors: the optical density (OD) of the *Agrobacterium* culture, co-cultivation time, and temperature for co-cultivation. These adjustments were made to avoid *Agrobacterium* overgrowth, minimize the duration of infection and enhance the efficiency of transformation. Additionally, we evaluated a more acidic pH of the media, as it has been associated with virulence gene induction and facilitation of T-DNA transfer (Yuan et al., 2008; Wang et al 2018).

To evaluate these parameters, we employed embryos derived from three distinct panicles. The infection procedure was applied uniformly to all embryos using a construct carrying Zm*Ubi*$_{pro}$::*GUS-intron* without the presence of morphogenic regulators. We tested different parameters during the experimentation: the OD of the *Agrobacterium* solution (0.3 and 0.7), co-cultivation incubation time (3 and 4 days), and incubation temperature (21 and 24 °C). Following the co-cultivation period of 3 or 4 days, embryos were transferred to resting media. Subsequently, 7 days after infection, GUS staining was carried out to assess the DNA delivery (Figure 1a-h). This time frame allowed for detection and visualization of the *GUS* gene expression, serving as an indicator of DNA transfer.

Despite the reported enhancement of *Agrobacterium* virulence under acidic pH conditions, our observations revealed that embryos subjected to pH 5.2 during co-cultivation exhibited reduced callus development and no detectable GUS expression (Figure 1a, c, e and g).

Following the quantification of *GUS* expression levels (Figure 1i-j), a discernible trend emerged: greater expression was observed at OD 0.3 compared to OD 0.7, and at 3 days compared to 4 days. Nonetheless, an elevation in temperature (21 vs 24 °C) did lead to a noticeable enhanced GUS expression level. However, it is worth noting that at 24 °C, favorable infection levels were achieved without encountering the anticipated problem of *Agrobacterium* overgrowth in the co-cultivation or resting period, which might occur if these cultures were maintained at 28 °C.

Hence, our optimized parameters for transformation rely on a pH value of 5.8 for co-cultivation, an *Agrobacterium* OD of 0.3 and 3 days of co-cultivation period at 24 °C (Figure 1f).

Morphogene-assisted transformation for efficient sorghum transformation.

The methodology consists of two fundamental components. The first component encompasses the excisable morphogenic gene cassette, with flanking loxP recombination sites, and three expression cassettes: *Axig1*$_{pro}$::*ZmWus2* and *Pltp*$_{pro}$::*ZmBbm* for morphogenic regulator expression, and *Glb1*$_{pro}$::*MoCRE* for recombinase expression, which facilitates cassette excision upon abscisic acid (ABA) induction. Notably, we employ non-constitutive promoters, maize phospholipid transferase protein promoter (*Pltp*$_{pro}$) driving *Bbm*, and auxin-inducible promoter (*Axig1*$_{pro}$) driving *Wus2*. The second component remains non-excised and houses the gene of interest (GOI), complete with its respective promoter and terminator, alongside the *nptII* selection marker (Figure 2a). It is noteworthy that the pVS1-VIR2 ternary vector, in conjunction with the *GRF4-GIF1* morphogenic regulator, has recently been documented to boost sorghum transformation efficiencies (Li et al., 2024). In line with this finding, we here utilized the pVS1-VIR2 ternary vector along with a compatible binary destination vector, pG3K-WO-AG harboring the morphogenic regulators *ZmBbm* and *ZmWus2* together with a GreenGate-compatible cloning site.

The transformation process follows the workflow illustrated in Figure 3. Initial steps involve a co-cultivation period, previously optimized to enhance *Agrobacterium* T-DNA integration, followed by a resting period. During both phases, the presence of 2,4-D induces the expression

of *Wus2*, initiating together with *Bbm* proembryo formation as early as 7 DAI (Figure 2c). Proembryos are characterized by the appearance of proliferative bulges at the scutellum epithelium (Wehbi et al., 2022). Notably, somatic embryo formation occurs as early as 14 DAI, with somatic embryos observed in the globular and scutellar stages (Figure 2d). Additionally, friable callus type II forms within the embryogenic tissue, where *GUS* expression is concentrated. During this stage, transgenic cell proliferation and the presence of somatic embryos in the coleoptilar stage are evident (Figure 2e).

Following somatic embryo induction, calli are sub-cultured on culture media containing G418 selection (100 mg/L). In this media, the presence of ABA induces *MoCRE* expression, further facilitating cassette excision. This step aims to maximize transgenic somatic embryos and excise morphogenic regulators, thereby facilitating transgenic embryo maturation and germination while minimizing non-transgenic embryo formation. The induction of excision at early somatic embryo stages allows for a substantial proportion of morphogenic regulator-free transgenic plantlets, achieving an excision efficiency of 67.7% based on one biological replicate (Table 1). After 14 days of sub-culture, the calli become highly friable, and a substantial number of somatic embryos have already germinated, exhibiting embryonic shoots and roots (Figure 2f). At this juncture, we increase the selection pressure (250 mg/L G418) to ensure transgenic shoot formation and minimize escape frequency, achieving an average escape frequency of 1% based on two biological replicates (Table 1).

Finally, germinated somatic embryos are transferred to rooting media, where they spend two weeks under light conditions, inducing root formation and chlorophyll accumulation (Figure 2g, h). The total duration of the protocol is reduced to 66 days (Figure 3), compared to the 12-16 weeks required by conventional *Agrobacterium* or particle bombardment-based methods that do not incorporate morphogenic regulators (Liu and Godwin, 2012; Zhao et al., 2000).

The optimization of infection conditions and the introduction of this novel sorghum transformation method, combining *Bbm* and *Wus2* morphogenic regulators together with the ternary vector pVS1-VIR2, have enabled us to achieve a highly efficient transformation protocol. We achieved transformation efficiencies of 28.3% (based on embryos producing at least one regenerated shoot) and 164.8% (based on the total number of isolated plantlets) (Table 1). Moreover, the adaptability of this vector system to include the Cas9 protein and guide RNAs within the GOI cassette opens up possibilities for producing marker/transgene-free genome edited plants, addressing emerging concerns regarding genetically modified organisms in accordance with European regulations.

Molecular and phenotypical characterization of regenerant plants.

To characterize the T0 plants, we employed digital PCR (dPCR) to assess T-DNA copy number, detect the presence of binary vector backbone, and monitor Cre/lox-mediated excision. Among the 45 independent T0 plants analyzed by dPCR, one plant was an escape, and five plants exhibited a T-DNA copy number of three or higher. Notably, 22 plants had a single T-DNA insertion without vector backbone, classifying them as high-quality events. Additionally, 15 of these 22 plants showed no presence of *MoCRE*, indicating complete excision of the morphogenic genes (Figure 6, Table S5).

Further phenotypic characterization was performed to investigate the role of morphogenic regulators driven by non-constitutive promoters in sorghum regenerant plants. As described by Lowe et al. (2018), using non-constitutive promoters (*Pltp*pro and *Axig1*pro) in maize restricted the expression of morphogenic regulators, enabling the generation of fertile plants without excision of the morphogenic regulator cassette. However, when we continued with phenotypic analysis of a sorghum regenerant plant carrying a single copy of the morphogenic regulator cassette, we still observed a pleiotropic phenotype, including an inability to produce flower organs (Figure 4b).

We cannot definitively attribute these effects solely to the morphogenic regulators due to concurrent overexpression of the studied GOI. However, overexpression of the GOI alone, without morphogenic regulators, resulted in the normal formation of flower organs. Nevertheless, panicle size was reduced in seven out of nine phenotypically characterized transgenic plants (Figure 4c, d). Next, we studied the phenotype of a transformation escape and ruled out any potential involvement of the transformation process in the observed phenotypes (Figure 4a).

The GOI used for these transformation events encodes a membrane-localized protein fused to GREEN FLUORESCENT PROTEIN (GFP). Prior to transferring to soil, GFP presence was confirmed by confocal microscopy to validate proper T-DNA expression. T0 plantlets carrying the T-DNA exhibited plasma membrane-localized GFP (Figure 4f), while no GFP signal was detected in non-transformed wild-type (WT) roots (Figure 4e).

In conclusion, excision of morphogenic regulators appears to be a necessary strategy to avoid unpredictable interactions with the GOI.

Combining pVS1-VIR2 with *ZmBbm* and *ZmWUS2* in maize

Inspired by this very successful transformation of sorghum, we decided to test the combination of the pVS1-VIR2 ternary vector and the pG3K-WO-ZmUbi$_{pro}$::*GUS*-intron:t*BdUBI1*-C binary vector in the maize inbred line B104, and compare it with a comparable binary vector without morphogenic genes, pG3K-ZmUbi$_{pro}$::*GUS*-intron:t*BdUBI1*-C. For transformation, we used the recently published protocol from Kang *et al*. in which they used the ternary vector pKL2299 in combination with geneticin selection to transform B104 to yield a 6.4% transformation frequency (Kang *et al*., 2022). Here, we transformed the binary vectors in an LBA4404 strain containing pVS1-VIR2 and used embryos of four ears. For each ear, approximately 50 embryos were used. Examination of transient *GUS* expression revealed all embryos expressing *GUS* (Figure 5a-b) with clear somatic embryo formation in the embryos transformed with the morphogenic genes (Figure 5b). This resulted in a marked increase in the number of regenerated plants (Figure 5c-d). While with the control construct seven transgenic plants (6 independent) from 210 starting embryos were obtained (3.3% transformation frequency), 110 (47 independent) transgenic plants out of 218 starting embryos were obtained with the combination of the pVS1-VIR2 ternary vector and pG3K-WO-ZmUbi$_{pro}$::GUS-intron:tBdUBI1-C (50.46% total transformation frequency, 21.6% independent transformation frequency). Next, we kept 33 plants for molecular characterization using dPCR and analyzed the presence of the *nptII* selection marker and the gentamycin resistance gene, present on the vector backbone, and the *MoCre* transgene, indicative of excision (Figure 6, Table S6). For the control, four out of six tested plants were high-quality events with a single T-DNA copy and no backbone (Table S6). For pG3K-WO-ZmUbi$_{pro}$::GUS-intron:tBdUBI1-C, one out of 27 tested T0 plants was found to be an escape, and nine plants had only a single T-DNA copy (Table S6). One of these plants had no evidence of *MoCre* presence and is considered as having the morphogenic genes excised (Table S6). We kept twelve several plants with a different morphogenic regulator copy number and evaluated phenotypes/fertility. All nine plants with one copy of *MoCre* present were fertile, while the three plants with five copies we retained had no, one and ample seeds respectively.

In conclusion, the combination of the ternary vector with pG3K-WO-ZmUbi$_{pro}$::GUS-intron:tBdUBI1-C also increased transformation frequency in maize 7-fold compared to the ternary alone, generating fertile plants with low T-DNA copy numbers

(V) DISCUSSION

Sorghum genetic transformation has historically faced challenges due to sorghum's recalcitrance and low regeneration frequency (Belide et al., 2017). The adoption of *Agrobacterium*-mediated transformation has significantly improved regeneration frequencies, becoming the predominant transformation protocol, as evidenced by studies conducted by Anand et al. (2018), Che et al. (2018), Hoerster et al. (2020), Che et al. (2022), Johnson et al. (2023), and Wang et al. (2023). A common practice in monocot transformation studies involves the utilization of LBA4404 Thy^- *Agrobacterium* strains. This thymidine auxotrophic strain needs thymidine for its growth and proves advantageous in preventing excessive *Agrobacterium* proliferation during co-cultivation stages. The restricted growth of *Agrobacterium*, attributable to the absence of thymidine during the resting period, may contribute to the prolonged co-cultivation periods and elevated *Agrobacterium* OD use in established sorghum transformation protocols. In this study, we optimized *Agrobacterium* infection by employing the EHA105 strain, which is readily accessible but lacks thymidine auxotrophy, thus lacking the growth-limiting advantage. Through optimization, we demonstrated that reducing the co-cultivation temperature to 24 °C—an intermediate temperature between common maize (21 °C) (Aesaert et al., 2022) and sorghum (28 °C) (Che et al., 2022) co-cultivation temperatures—and decreasing the co-cultivation duration to 3 days—a timeframe more akin to maize transformation protocols (Aesaert et al., 2022) compared to the 7 days typically employed in sorghum transformation procedures (Aregawi et al., 2022)—effectively mitigates *Agrobacterium* overgrowth, facilitating proper tissue culture. These adjustments align more closely with the framework employed in the latest published transformation protocols, further reinforcing the notion that reduced temperatures and incubation times are adequate for efficient *Agrobacterium* DNA delivery (Li et al., 2024). Further standardization of *Agrobacterium* infection revealed that, contrary to the reported enhancement of *Agrobacterium* virulence under acidic pH (Yuan et al., 2008; Wang et al., 2018), embryos subjected to a pH of 5.2 exhibited reduced callus development and no detectable *GUS* expression (Figure 1a, c, e, g). This indicates that pH is a limiting factor in sorghum callus cell proliferation and that a more acidic pH negatively impacts the viability of the plant material.

It is important to highlight that in the morphogene-based transformation system, we strategically incorporated morphogenic regulators, specifically *Bbm* and *Wus2*, known for their pivotal role in promoting somatic embryogenesis (Zuo et al., 2002; Lowe et al., 2016; Horstman et al., 2017; Chen et al., 2022). These regulators were driven by non-constitutive promoters:

the maize phospholipid transferase protein promoter ($Pltp_{pro}$) for *Bbm* and the auxin-inducible promoter ($Axig1_{pro}$) for *Wus2*. This approach, proven effective in inducing somatic embryogenesis in maize (Jones et al., 2019), was tailored to enhance the somatic embryogenesis process in our sorghum transformation protocol.

By integrating these morphogenic regulators into the protocol, we significantly streamlined the transformation process, reducing the total duration to just 66 days. This represents a substantial improvement over conventional methods, such as *Agrobacterium* or particle-bombardment-based techniques that do not incorporate morphogenic regulators (Liu and Godwin, 2012; Zhao et al., 2000).

For maize B104, we obtained a transformation frequency of 3,3% when using the control vector pG3K-ZmUbi$_{pro}$::GUS-intron:tBdUBI1-C together with the LBA4404 strain equipped with ternary helper vector pVS1-VIR2 and G418-based selection. This is less compared to the average 6.4% B104 transformation frequency obtained using the LBA4404 strain equipped with the ternary helper vector pKL2299 and selection using G418 (Kang *et al*., 2022) and less compared to the average 8.2% B104 transformation frequency we observed when using the strain EHA105 recA^{-}, pVS1-VIR2 and selection using hygromycin (Vandeputte *et al*., 2024). We anticipate that with optimization of the protocol (infection, tissue culture) we will be able to further improve the frequency. Similar to sorghum, combining with *Bbm* and *Wus2*, led to a drastic increase in transformation efficiency, reaching up to 21.6%. Previously, we observed that maize T0 plants containing high copy numbers of *Axig1*pro::*ZmWus2* and *Pltp*pro::*ZmBbm* were associated with pleiotropic effects (Aesart *et al*., 2022). Remarkably, only five of the 27 tested plants transformed with pG3K-WO-ZmUbi$_{pro}$::GUS-intron:tBdUBI1-C had a T-DNA copy number greater than two. Excision was less efficient compared to sorghum with only four lines showing absence of the morphogenic gene cassette (Figure 6). In other lines excision was absent or only partial. We here use the promoter of the late-embryogenesis and ABA-inducible maize gene *GLOBULIN-1* (Duncan et al., 2003) to drive *MoCRE* expression. Further optimization of timing and concentration of ABA during the process or use of alternative promoters to drive *MoCRE* expression may aid to improve this step in the future for maize. Nevertheless, as all plants are fertile, pG3K-WO-AG can be used for gene editing approaches in which the T-DNA and morphogenic genes are crossed out.

In the sorghum transformation methodology, we combined the ternary vector pVS1-VIR2 with *Bbm* and *Wus2*, setting it apart from previous protocols and significantly boosts efficiency. We have achieved a remarkable enhancement in total transformation efficiency, reaching up to

164.8%, a 2.36-fold increase compared to the highest sorghum transformation efficiency reported (Che et al., 2022). Notably, Li et al., 2024, recently achieved transformation efficiencies of 39.68%, based on embryos producing at least one regenerated shoot, using a similar combination of *GRF4-GIF1* with pVS1-VIR2, which closely aligns with our own achievement of 30.8% transformation efficiency with *Bbm* and *Wus2*.

Our highly efficient sorghum transformation method represents a significant advancement for plant biotechnology, particularly within the European scientific community. However, it is important to note that the Tx430 genotype, while well-established since the early 1990s (Casas et al., 1993), is not representative of modern or globally significant sorghum parental lines. Future work should aim to extend this method to elite varieties, such as Macia (SDS 3220), widely grown across Africa (Wanga et al., 2023), and Tx623, the reference genome sequence (Paterson et al., 2009). Other key targets include dominant genotypes like M35-1 in India (Rama Reddy et al., 2014), and European-adapted varieties (Schaffasz et al., 2019). The routine transformation of these genotypes would greatly enhance sorghum biotechnology's global impact and accelerate breeding programs for widely cultivated elite varieties.

(VI) EXPERIMENTAL PROCEDURES

Sorghum transformation

The transformation method, illustrated in Figure 2, is described in detail in the following sections.

Collecting immature embryos from Tx430 sorghum plants.

Fifteen days after anthesis initiation, embryos were selected based on size, ranging from 1.5 to 2 mm (Figure 2b). Spikelets containing embryos of the specified size were harvested and each seed was carefully separated by hand to avoid damage, which facilitated embryo isolation. The individual seeds were then placed in 50 ml conical centrifuge tubes and stored at 4 °C overnight.

***Agrobacterium* preparation.**

A schematic representation of the construct used in this work is provided in Figure 2a. Two different GOI constructs were employed: $ZmUbi_{pro}$::GUS-intron-tBdUbi1-C, used to monitor *Agrobacterium* infection and stable expression throughout the transformation stages, and

$ZmUbi_{pro}$::(Membrane-localized protein fused to GFP)-tBdUbi1-C, utilized to obtain overexpressor lines. A glycerol stock of *Agrobacterium* strain EHA105 $recA^-$ carrying the pVS1-VIR2 and the specified constructs was used to inoculate a plate with YP media (Table S1) and incubated at 28 °C in the dark for 3 days. One day before transformation, actively growing *Agrobacterium* was used to inoculate a freshly prepared YP media plate and incubated at 28 °C in the dark overnight. On the day of transformation, a scoop of *Agrobacterium* was mixed in a 50 ml conical centrifuge tube containing 10 ml of Infection media (Table S1) and the mixture was incubated at room temperature in a horizontal shaker at 200 rpm for a minimum of 2 hours.

Sorghum seed sterilization and isolation of immature embryos.

Seeds were sterilized in 50 ml conical centrifuge tubes by adding 5% bleach and placing the tubes on a rotor wheel for 20 minutes. The seeds were then washed with sterile distilled water for 5 minutes in the rotor wheel, repeating this process five times. The sterilized seeds were placed in large petri dishes and embryos were isolated using tweezers and a dissecting lancet (Figure S1). The isolated embryos were then placed in a 2 ml microcentrifuge tube containing 1.75 ml of Infection media with 25 embryos per tube.

Infection, co-cultivation and resting.

Embryos were washed by removing all the Infection media from the tubes and adding 1 ml of fresh Infection media. The tubes were inverted 3-4 times, and the Infection media was pipetted off; this step was repeated. Following this, 1 ml of *Agrobacterium* solution was added. Before use, the *Agrobacterium* solution was diluted in Infection media to an OD of 0.3 at 550 nm wavelength. The tube was inverted 20 times and incubated at room temperature in the dark for 5 minutes. Subsequently, 500 µl of the *Agrobacterium* solution was removed and the remaining solution was poured into a petri dish with Co-cultivation media (Table S1). Excess *Agrobacterium* solution was removed with a pipette and the embryos were placed scutellum side up and evenly distributed. The plates were then sealed with micropore tape and incubated at 24 °C in the dark for 3 days. After this incubation period, the embryos were transferred to a new petri dish containing Resting media (Table S1) to induce callus formation and were incubated at 26 °C in the dark for 7 days. A checkpoint was included to monitor transient

expression by performing histochemical staining with X-Gluc (GUS staining) 7 days after infection (DAI) (Figure 2c).

Induction of somatic embryogenesis with Maturation media I

After resting for 7 days, the embryos that had started to form callus were transferred to Maturation media I (Table S1). The radicle was removed using a scalpel and tweezers. They were incubated at 26 °C in the dark for 12 days and non-progressed embryos were discarded. At 14 DAI, the calli were used for GUS staining. The first GUS staining provided information about the infection efficiency of the transformation, although it could still reflect transient expression. In the second GUS staining, stable expression of the transgene was studied. In the case of stable expression, a transition from single-cell expression to cell clusters containing the transgene can be observed. Embryogenic tissue formation can also already be evaluated at this point (Figure 2d).

Regeneration and rooting

After 12 days in Maturation media I, all calli were transferred to Maturation media II (Table S1) containing 100 mg/L of geneticin (G418, Gibco, Thermo Fisher Scientific; Waltham, MA, USA). They were incubated at 26 °C in the dark for 14 days. At 21 DAI, the calli were used for GUS staining. After 7 days in Maturation media II, the selection effect on non-transformed cells was already visible as necrotic tissue. However, clusters of living cells expressing the construct were a good indication of stable expression of the construct, including the selecting agent (Figure 2e).

After 14 days on Maturation media II, regenerated plantlets can already be observed (Figure 2f). The callus and regenerant plants were transferred to fresh Maturation media II with 250 mg/L of geneticin. Since the callus was very friable at this stage, care was taken during subculturing and the callus was divided into several pieces to allow proper growth of the regenerant plants. The regenerant plants and embryogenic tissue from the same callus were tracked to differentiate putative clonal plants with the inserted T-DNA in the same genomic region. As the calli grew and were divided into more pieces, they occupied more space, around 10-12 calli were placed per plate.

After 14 days, the calli and regenerant plants were transferred to Rooting media (Table S1) and incubated at 25 °C with a light regime of 80-100 µE/m²/s light intensity in a 16:8 cycle until the roots were well formed. After 14 days in Rooting media, the shoots turned green and elongated, and primary and secondary roots formed and elongated (Figure 2g, h).

Passing to soil T0 plants

The rooted plantlets were then transferred to soil using pre-wetted Jiffy-7 pellets and covered with a plastic box to maintain high humidity, aiding in their acclimatization from tissue culture to soil. These transgenic plantlets were maintained under controlled growth conditions, with a light intensity of 300 µE/m²/s, a 16-hour light period at 26 °C, and an 8-hour dark period at 22 °C. The humidifying cover was removed after 3 days.

Genotyping and determining quality events.

Stable T-DNA integration was determined by PCR using genomic DNA extracted from T0 plantlet leaves. Different PCRs were performed to test the presence of the GOI and the presence of the non-excised morphogenic regulators (Figure S2). The primers used in this study are specified in Table S2. The quality events (presence of *nptII* and absence of *MoCRE* and *GmR* [binary vector backbone]) were further analyzed by dPCR to also determine the number of T-DNA copies (Table S5).

Vector construction

The *Sorghum bicolor UBIQUITIN* promoter (pSb*UBI*), *NEOMYCIN PHOSPHOTRANSFERASE II* coding sequence (*nptII*), and Sb*UBI* terminator (tSb*UBI*) were ordered as synthetic DNA flanked by GreenGate AC, CD and DE sites respectively (Table S3, Twist Bioscience, South San Francisco, CA, USA) based on the vector PHP97334 (Wang *et al.* 2023). These elements were combined into GGIB shuttle vector pGGIB-U8-AG-9 using Golden Gate cloning (Lampropoulos *et al.*, 2013) to yield pGGIB-U8-pSbUBI-nptII-tSbUBI-U9 and subsequently combined using Gibson assembly with pGGIB-U1-linker-U7 and pGGIB-U7-A-BsaI-sfGFP-BsaI-G-U8 in a destination vector

pG3-U1-AG-U9 (Vandeputte *et al*., 2024), which is compatible with pVS1-VIR2. This yielded the new Golden Gate-compatible destination vector pG3K-AG. For a novel destination vector with the morphogenic genes, a Gibson assembly reaction was set up using pGGIB-U1-LoxP-U2, pGGIB-U2-pZmGLB1-*MoCre*-tnos-U3, pGGIB-U3-pZmAXIG1-ZmWUS2-t35S-U4, pGGIB-U4-pZmPLTP-ZmBBM-tnos-U5, pGGIB-U5-LoxP-U6, pGGIB-U6-A-BsaI-sfGFP-BsaI-G-U7, pGGIB-U7-linker-U8 and pGGIB-U8-pSbUBI-nptII-tSbUBI-U9 in the vector pG3-U1-AG-U9 (Aesaert *et* al., 2022, Vandeputte *et al*., 2024). This yielded the destination vector pG3K-WO-AG. These destination vectors where subsequently used to create the expression vectors pG3K-ZmUbi$_{pro}$::GUS-intron:tBdUBI1-C and pG3K-WO-ZmUbi$_{pro}$::GUS-intron:tBdUBI1-C using Golden Gate cloning. All destination and expression vectors were verified using whole plasmid sequencing (Eurofins). All vectors and vector maps (.gb files) are available from the VIB plasmid repository https://vectorvault.vib.be/. The ternary vector pVS1-VIR2 (Zhang et al., 2019) is available from addgene.org as plasmid #134745."

Maize transformation

The constructs pG3K-ZmUbi$_{pro}$::GUS-intron:tBdUBI1-C and pG3K-WO-ZmUbi$_{pro}$::GUS-intron:tBdUBI1-C , also used for Sorghum transformation were transformed in the strain LBA4404 containing the pVS1-VIR2 ternary vector. The method for transformation was essentially as described (Kang et al., 2022). Four independent ears of B104 were used with twelve-day-old embryos, stored overnight at 4°C before embryo isolation. For each cob, approximately 50 embryos were used totaling between 199 and 218 per experimental condition. *Agrobacterium* were grown over the weekend on AB-medium with appropriate selection. On Monday, bacteria were resuspended in 100 µl H_2O and plated on YP-plates with antibiotics. LBA4044 cells were resuspended from plate in 7 mL infection medium with AS and diluted in new infection media to OD_{550} of 0.50. Embryos were incubated on maize co-cultivation medium (pH 5.6) for 1 day at 21 °C in the dark and progressed in tissue culture as described (Kang et al., 2022).

Digital PCR

We used nanoplate-based digital PCR (dPCR) for molecular characterization of T0 events. Genomic DNA (gDNA) was prepared using the Wizard® Genomic DNA Purification kit (Promega) and quantified using the Qubit dsDNA HS Assay Kit (Thermo Fisher Scientific: Waltham, MA,

USA). For maize and sorghum, gDNA was diluted to 5 and 2 ng/µL respectively. After adding primers, probes (Table S2) and the QIAcuity Probe PCR Kit Master Mix (Qiagen,: Germantown, MD, USA) mixtures were digested with CviQI (NEB) for 10 min at 24 °C. The Qiagen QIAcuity One 5-plex platform and an 8.5K 24-well or 96-well Nanoplate was used. Probes (PrimeTime™, IDT, Leuven, Belgium) contained 6-FAM, HEX and Cy5 fluorophores for selection marker, reference gene and backbone, respectively. Single-copy reference genes *FPGS* (Zm00007a00000670) for maize (Manoli et al., 2012) or Sb*ENOL1* (SORBI_3002G186900) for sorghum (Belide et al., 2017) were used.

GUS staining and quantification

Calli were harvested and incubated in 90% acetone at 4 °C for 30 min. After removing the acetone, the calli were incubated in phosphate buffer (50 mM NaPO4, 0.01% Triton, pH 7) at room temperature with shaking. Subsequently, the buffer was replaced with cyanide buffer (2 mM ferricyanide, 2 mM ferrocyanide in phosphate buffer) and incubated for 30 min under vacuum followed by 30 min at 37 °C. The cyanide buffer was then replaced with X-Gluc solution (3 mM X-Gluc [Duchefa; Haarlem, Netherlands] in cyanide buffer), and the calli were incubated at 37 °C for 30 min. Following this, the calli were washed with phosphate buffer and photographed. *GUS* expression was quantified by measuring the percentage of stained area using GIMP software, with blue pixels selected using the color selection tool and compared to the total pixels.

Statistical analysis

Data were analyzed using a two-way Analysis of Variance (ANOVA) followed by Tukey's Honestly Significant Difference (HSD) test. Differences between group means were considered statistically significant if the p-value was less than 0.05. Results are presented with different letters indicating statistically significant differences between groups. Groups sharing the same letter are not significantly different, while groups with different letters are significantly different.

(VII) ACCESSION NUMBERS

This article does not contain sequences in any repository.

(VIII) ACKNOWLEDGMENTS

This project has received funding from the European Research Council (ERC) under the European Union's Horizon 2020 research and innovation programme (grant agreement No 683163). Juan B. Fontanet-Manzaneque has been funded by European Research Council (ERC) under the European Union's Horizon 2020 research and innovation programme (grant agreement No 683163) awarded to Ana I. Caño-Delgado and by Grant PID2020-118218RB-I00 funded by MCIU/AEI/10.13039/501100011033. Juan B. Fontanet-Manzaneque was additionally supported by EMBO Scientific Exchange Grant (number 9889)

The authors have no conflicts of interest to declare.

(IX) SHORT LEGENDS FOR SUPPORTING INFORMATION

Table S1. Medium composition for sorghum transformation.

Table S2. Oligonucleotides used in this study.

Table S3. DNA sequences of elements synthesized in this study. *BsaI* restriction sites are indicated in red, GreenGate overhang in green, and start- and stop codons in blue.

Table S4. Plasmids used in this study. *KmR*, kanamycin resistance; *GmR*, gentamycin resistance; sf*GFP*, PglpT-sfGFP-TrrfB visual marker for E. coli.

Table S5. Molecular characterization of sorghum T0 plants using digital PCR. Copy numbers of the selection marker (*nptII*) and vector backbone (*GmR*) were determined using dPCR. Presence of the *MoCRE* gene was used to examine Cre/lox-mediated excision of the morphogenic genes.

Table S6. Molecular characterization of maize T0 plants using digital PCR. Copy numbers of the selection marker (*nptII*) and vector backbone (*GmR*) were determined using dPCR. Presence of the *MoCRE* gene was used to examine Cre/lox-mediated excision of the morphogenic genes. When multiple plants were derived from the same immature embryo they are given an additional lowercase letter.

Figure S1: Immature sorghum embryo isolation procedure. (a) Position the seed with tweezers, ensuring the embryo side (opposite the hilum) is facing upward. (b) Use a lancet to create a small aperture at the tip of the seed. (c) Gently press the lancet at the bottom of the seed, taking care to avoid damaging the embryo. (d) Extract the embryo with the tip of the lancet and transfer it into microcentrifuge tubes.

Figure S2. Gel electrophoresis of amplified DNA by PCR in transgenic and non-transgenic (WT) plants. Plasmid DNA was also amplified as a positive control. The amplicon length is 663 bp for the GOI region and 1133 bp for the excision cassette region.

(X) REFERENCES

Aesaert S, Impens L, Coussens G, Van Lerberge E, Vanderhaeghen R, Desmet L, Vanhevel Y, Bossuyt S, Wambua AN, Van Lijsebettens M, Inzé D, De Keyser E, Jacobs TB, Karimi M, Pauwels L. Optimized Transformation and Gene Editing of the B104 Public Maize Inbred by Improved Tissue Culture and Use of Morphogenic Regulators. Front Plant Sci. 2022 Apr 22;13:883847. doi: 10.3389/fpls.2022.883847. PMID: 35528934; PMCID: PMC9072829.

Aliu E, Ji Q, Wlazlo A, Grosic S, Azanu MK, Wang K, Lee K. Enhancing *Agrobacterium*-mediated plant transformation efficiency through improved ternary vector systems and auxotrophic strains. Front Plant Sci. 2024 Jul 23;15:1429353. doi: 10.3389/fpls.2024.1429353. PMID: 39109064; PMCID: PMC11300283.

Anand A, Bass SH, Wu E, Wang N, McBride KE, Annaluru N, Miller M, Hua M, Jones TJ. An improved ternary vector system for *Agrobacterium*-mediated rapid maize transformation. Plant Mol Biol. 2018 May;97(1-2):187-200. doi: 10.1007/s11103-018-0732-y. Epub 2018 Apr 23. PMID: 29687284; PMCID: PMC5945794.

Aregawi K, Shen J, Pierroz G, Sharma MK, Dahlberg J, Owiti J, Lemaux PG. Morphogene-assisted transformation of Sorghum bicolor allows more efficient genome editing. Plant Biotechnol J. 2022 Apr;20(4):748-760. doi: 10.1111/pbi.13754. Epub 2021 Dec 16. PMID: 34837319; PMCID: PMC8989502.

Belide S, Vanhercke T, Petrie JR, Singh SP. Robust genetic transformation of sorghum (*Sorghum bicolor* L.) using differentiating embryogenic callus induced from immature embryos. Plant Methods. 2017 Dec 8;13:109. doi: 10.1186/s13007-017-0260-9. PMID: 29234458; PMCID: PMC5723044.

Casas AM, Kononowicz AK, Zehr UB, Tomes DT, Axtell JD, Butler LG, Bressan RA, Hasegawa PM. Transgenic sorghum plants via microprojectile bombardment. Proc Natl Acad Sci U S A. 1993 Dec 1;90(23):11212-6. doi: 10.1073/pnas.90.23.11212. PMID: 8248230; PMCID: PMC47952.

Che P, Anand A, Wu E, Sander JD, Simon MK, Zhu W, Sigmund AL, Zastrow-Hayes G, Miller M, Liu D, Lawit SJ, Zhao ZY, Albertsen MC, Jones TJ. Developing a flexible, high-efficiency *Agrobacterium*-mediated sorghum transformation system with broad application. Plant Biotechnol J. 2018 Jul;16(7):1388-1395. doi: 10.1111/pbi.12879. Epub 2018 Feb 6. PMID: 29327444; PMCID: PMC5999184.

Che P, Wu E, Simon MK, Anand A, Lowe K, Gao H, Sigmund AL, Yang M, Albertsen MC, Gordon-Kamm W, Jones TJ. Wuschel2 enables highly efficient CRISPR/Cas-targeted genome editing during rapid de novo shoot regeneration in sorghum. Commun Biol. 2022 Apr 11;5(1):344. doi: 10.1038/s42003-022-03308-w. PMID: 35410430; PMCID: PMC9001672.

Chen B, Maas L, Figueiredo D, Zhong Y, Reis R, Li M, Horstman A, Riksen T, Weemen M, Liu H, Siemons C, Chen S, Angenent GC, Boutilier K. BABY BOOM regulates early embryo and endosperm development. Proc Natl Acad Sci U S A. 2022 Jun 21;119(25):e2201761119. doi: 10.1073/pnas.2201761119. Epub 2022 Jun 16. PMID: 35709319; PMCID: PMC9231476.

Duncan, D. R., Kriz, A. L., Paiva, R., & Widholm, J. M. (2003). Globulin-1 gene expression in regenerable *Zea mays* (maize) callus. Plant cell reports, 21, 684-689.

Food and Agriculture Organization of the United Nations. FAOSTAT Statistical Database. [Rome]: FAO, 2022.

Gordon-Kamm B, Sardesai N, Arling M, Lowe K, Hoerster G, Betts S, Jones AT. Using Morphogenic Genes to Improve Recovery and Regeneration of Transgenic Plants. Plants (Basel). 2019 Feb 11;8(2):38. doi: 10.3390/plants8020038. PMID: 30754699; PMCID: PMC6409764.

Hoerster, G., Wang, N., Ryan, L., Wu, E., Anand, A., McBride, K., Lowe, K. et al. (2020) Use of non-integrating Zm-Wus2 vectors to enhance maize transformation. In Vitro Cell. Dev. Biol. Plant, 56, 265–279. doi: 10.1007/s11627-019-10042-2

Horstman A, Li M, Heidmann I, Weemen M, Chen B, Muino JM, Angenent GC, Boutilier K. The BABY BOOM Transcription Factor Activates the LEC1-ABI3-FUS3-LEC2 Network to Induce Somatic Embryogenesis. Plant Physiol. 2017 Oct;175(2):848-857. doi: 10.1104/pp.17.00232. Epub 2017 Aug 22. PMID: 28830937; PMCID: PMC5619889.

Johnson K, Cao Chu U, Anthony G, Wu E, Che P, Jones TJ. Rapid and highly efficient morphogenic gene-mediated hexaploid wheat transformation. Front Plant Sci. 2023 Mar 29;14:1151762. doi: 10.3389/fpls.2023.1151762. PMID: 37063202; PMCID: PMC10090459.

Jones T, Lowe K, Hoerster G, Anand A, Wu E, Wang N, Arling M, Lenderts B, Gordon-Kamm W. Maize Transformation Using the Morphogenic Genes Baby Boom and Wuschel2. Methods Mol Biol. 2019;1864:81-93. doi: 10.1007/978-1-4939-8778-8_6. PMID: 30415330.

Kang M, Lee K, Finley T, Chappell H, Veena V, Wang K. An Improved *Agrobacterium*-Mediated Transformation and Genome-Editing Method for Maize Inbred B104 Using a Ternary Vector System and Immature Embryos. Front Plant Sci. 2022 May 4;13:860971. doi: 10.3389/fpls.2022.860971. PMID: 35599865; PMCID: PMC9114882.

Kang M, Lee K, Ji Q, Grosic S, Wang K. Enhancing Maize Transformation and Targeted Mutagenesis through the Assistance of Non-Integrating *Wus2* Vector. Plants (Basel). 2023 Jul 28;12(15):2799. doi: 10.3390/plants12152799. PMID: 37570953; PMCID: PMC10420852.

Lampropoulos A, Sutikovic Z, Wenzl C, Maegele I, Lohmann JU, Forner J. GreenGate---a novel, versatile, and efficient cloning system for plant transgenesis. PLoS One. 2013 Dec 20;8(12):e83043. doi: 10.1371/journal.pone.0083043. PMID: 24376629; PMCID: PMC3869738.

Li J, Pan W, Zhang S, Ma G, Li A, Zhang H, Liu L. A rapid and highly efficient sorghum transformation strategy using GRF4-GIF1/ternary vector system. Plant J. 2024 Mar;117(5):1604-1613. doi: 10.1111/tpj.16575. Epub 2023 Dec 1. PMID: 38038993.

Liu G, Godwin ID. Highly efficient sorghum transformation. Plant Cell Rep. 2012 Jun;31(6):999-1007. doi: 10.1007/s00299-011-1218-4. Epub 2012 Jan 11. PMID: 22234443; PMCID: PMC3351618.

Lowe K, Wu E, Wang N, Hoerster G, Hastings C, Cho MJ, Scelonge C, Lenderts B, Chamberlin M, Cushatt J, Wang L, Ryan L, Khan T, Chow-Yiu J, Hua W, Yu M, Banh J, Bao Z, Brink K, Igo E, Rudrappa B, Shamseer PM, Bruce W, Newman L, Shen B, Zheng P, Bidney D, Falco C, Register J, Zhao ZY, Xu D, Jones T, Gordon-Kamm W. Morphogenic Regulators Baby

boom and Wuschel Improve Monocot Transformation. Plant Cell. 2016 Sep;28(9):1998-2015. doi: 10.1105/tpc.16.00124. Epub 2016 Sep 6. PMID: 27600536; PMCID: PMC5059793.

Lowe K, La Rota M, Hoerster G, Hastings C, Wang N, Chamberlin M, Wu E, Jones T, Gordon-Kamm W. Rapid genotype "independent" *Zea mays* L. (maize) transformation via direct somatic embryogenesis. In Vitro Cell Dev Biol Plant. 2018;54(3):240-252. doi: 10.1007/s11627-018-9905-2. Epub 2018 Apr 30. PMID: 29780216; PMCID: PMC5954046.

Manoli A, Sturaro A, Trevisan S, Quaggiotti S, Nonis A. Evaluation of candidate reference genes for qPCR in maize. J Plant Physiol. 2012 May 15;169(8):807-15. doi: 10.1016/j.jplph.2012.01.019. Epub 2012 Mar 27. PMID: 22459324.

Miller S, Rønager A, Holm R, Fontanet-Manzaneque JB, Caño-Delgado AI, Bjarnholt N. New methods for sorghum transformation in temperate climates. AoB Plants. 2023 Jun 3;15(3):plad030. doi: 10.1093/aobpla/plad030. PMID: 37396498; PMCID: PMC10308921.

Mullet JE, Klein RR, Klein PE. Sorghum bicolor - an important species for comparative grass genomics and a source of beneficial genes for agriculture. Curr Opin Plant Biol. 2002 Apr;5(2):118-21. doi: 10.1016/s1369-5266(02)00232-7. PMID: 11856606.

Ortiz D, Salas-Fernandez MG. Dissecting the genetic control of natural variation in sorghum photosynthetic response to drought stress. J Exp Bot. 2022 May 23;73(10):3251-3267. doi: 10.1093/jxb/erab502. PMID: 34791180; PMCID: PMC9126735.

Paterson AH, Bowers JE, Bruggmann R, Dubchak I, Grimwood J, Gundlach H, Haberer G, Hellsten U, Mitros T, Poliakov A, Schmutz J, Spannagl M, Tang H, Wang X, Wicker T, Bharti AK, Chapman J, Feltus FA, Gowik U, Grigoriev IV, Lyons E, Maher CA, Martis M, Narechania A, Otillar RP, Penning BW, Salamov AA, Wang Y, Zhang L, Carpita NC, Freeling M, Gingle AR, Hash CT, Keller B, Klein P, Kresovich S, McCann MC, Ming R, Peterson DG, Mehboob-ur-Rahman, Ware D, Westhoff P, Mayer KF, Messing J, Rokhsar DS. The Sorghum bicolor genome and the diversification of grasses. Nature. 2009 Jan 29;457(7229):551-6. doi: 10.1038/nature07723. PMID: 19189423.

Rama Reddy NR, Ragimasalawada M, Sabbavarapu MM, Nadoor S, Patil JV. Detection and validation of stay-green QTL in post-rainy sorghum involving widely adapted cultivar, M35-1 and a popular stay-green genotype B35. BMC Genomics. 2014 Oct 18;15(1):909. doi: 10.1186/1471-2164-15-909. PMID: 25326366; PMCID: PMC4219115.

Rodrigues SD, Karimi M, Impens L, Van Lerberge E, Coussens G, Aesaert S, Rombaut D, Holtappels D, Ibrahim HMM, Van Montagu M, Wagemans J, Jacobs TB, De Coninck B, Pauwels L. Efficient CRISPR-mediated base editing in *Agrobacterium* spp. Proc Natl Acad Sci U S A. 2021 Jan 12;118(2):e2013338118. doi: 10.1073/pnas.2013338118. Epub 2020 Dec 21. PMID: 33443212; PMCID: PMC7812762.

Schaffasz, A., Windpassinger, S., Friedt, W., Snowdon, R., & Wittkop, B. (2019). Sorghum as a novel crop for Central Europe: Using a broad diversity set to dissect temperate-adaptation. *Agronomy*, *9*(9), 535. doi: 10.3390/agronomy9090535

Vandeputte W., Coussens G., Aesaert S., Haeghebaert J., Impens L., Karimi, M, Debernardi J. and Pauwels L. (2024) Use of GRF-GIF chimeras and a ternary vector system to improve maize (Zea mays L.) transformation frequency. The Plant Journal (acccepted) doi: 10.1111/tpj.16880

Visarada K, Kishore NS. Advances in genetic transformation. In: Madhusudhana R, Rajendrakumar P, Patil JV, editors. Sorghum molecular breeding. New Delhi: Springer; 2015. pp. 199–215.

Wang N, Ryan L, Sardesai N, Wu E, Lenderts B, Lowe K, Che P, Anand A, Worden A, van Dyk D, Barone P, Svitashev S, Jones T, Gordon-Kamm W. Leaf transformation for efficient random integration and targeted genome modification in maize and sorghum. Nat Plants. 2023 Feb;9(2):255-270. doi: 10.1038/s41477-022-01338-0. Epub 2023 Feb 9. PMID: 36759580; PMCID: PMC9946824.

Wang YC, Yu M, Shih PY, Wu HY, Lai EM. Stable pH Suppresses Defense Signaling and is the Key to Enhance *Agrobacterium*-Mediated Transient Expression in Arabidopsis Seedlings. Sci Rep. 2018 Nov 20;8(1):17071. doi: 10.1038/s41598-018-34949-9. PMID: 30459348; PMCID: PMC6244089.

Wanga, M. A., Shimelis, H., Mashilo, J., Horn, L. N., & Sarsu, F. (2023). Responses of elite sorghum (Sorghum bicolor [L.] Moench) lines developed via gamma-radiation for grain yield, component traits and drought tolerance. Reproduction and Breeding, 3(4), 184-196. doi: 10.1016/j.repbre.2023.10.005

Wehbi H, Soulhat C, Morin H, Bendahmane A, Hilson P, Bouchabké-Coussa O. One-Week Scutellar Somatic Embryogenesis in the Monocot Brachypodium distachyon. Plants (Basel). 2022 Apr 14;11(8):1068. doi: 10.3390/plants11081068. PMID: 35448796; PMCID: PMC9025947.

Xie P, Tang S, Chen C, Zhang H, Yu F, Li C, Wei H, Sui Y, Wu C, Diao X, Wu Y, Xie Q. Natural variation in Glume Coverage 1 causes naked grains in sorghum. Nat Commun. 2022 Feb 25;13(1):1068. doi: 10.1038/s41467-022-28680-3. PMID: 35217660; PMCID: PMC8881591.

Yuan ZC, Liu P, Saenkham P, Kerr K, Nester EW. Transcriptome profiling and functional analysis of *Agrobacterium* tumefaciens reveals a general conserved response to acidic conditions (pH 5.5) and a complex acid-mediated signaling involved in *Agrobacterium*-plant interactions. J Bacteriol. 2008 Jan;190(2):494-507. doi: 10.1128/JB.01387-07. Epub 2007 Nov 9. PMID: 17993523; PMCID: PMC2223696.

Yue J, VanBuren R, Liu J, Fang J, Zhang X, Liao Z, Wai CM, Xu X, Chen S, Zhang S, Ma X, Ma Y, Yu H, Lin J, Zhou P, Huang Y, Deng B, Deng F, Zhao X, Yan H, Fatima M, Zerpa-Catanho D, Zhang X, Lin Z, Yang M, Chen NJ, Mora-Newcomer E, Quesada-Rojas P, Bogantes A, Jiménez VM, Tang H, Zhang J, Wang ML, Paull RE, Yu Q, Ming R. SunUp and Sunset genomes revealed impact of particle bombardment mediated transformation and domestication history in papaya. Nat Genet. 2022 May;54(5):715-724. doi: 10.1038/s41588-022-01068-1. Epub 2022 May 12. PMID: 35551309.

Zhang Q, Zhang Y, Lu MH, Chai YP, Jiang YY, Zhou Y, Wang XC, Chen QJ. A Novel Ternary Vector System United with Morphogenic Genes Enhances CRISPR/Cas Delivery in Maize. Plant Physiol.

2019 Dec;181(4):1441-1448. doi: 10.1104/pp.19.00767. Epub 2019 Sep 26. PMID: 31558579; PMCID: PMC6878030.

Zhao ZY, Cai T, Tagliani L, Miller M, Wang N, Pang H, Rudert M, Schroeder S, Hondred D, Seltzer J, Pierce D. *Agrobacterium*-mediated sorghum transformation. Plant Mol Biol. 2000 Dec;44(6):789-98. doi: 10.1023/a:1026507517182. PMID: 11202440.

Zuo J, Niu QW, Frugis G, Chua NH. The WUSCHEL gene promotes vegetative-to-embryonic transition in Arabidopsis. Plant J. 2002 May;30(3):349-59. doi: 10.1046/j.1365-313x.2002.01289.x. PMID: 12000682.

(XI) TABLES

Table 1. Transformation efficiency, escape frequency and excision efficiency in sorghum transformation protocol. a) Embryos with at least one regenerated shoot/starting embryos. b) Total isolated individual plantlets/starting embryos. c) Total number of escapes/starting embryos. d) Plantlets without *MoCRE* gene/ plantlets analyzed by PCR

(XII) FIGURE LEGENDS

Figure 1. GUS-stained calli and quantification for optimization of infection conditions. (a-h) GUS-stained calli with different condition of pH, Optical density, and temperature. (a) pH 5.2, OD 0.3 and 21°C. (b) pH 5.8, OD 0.3 and 21°C. (c) pH 5.2, OD 0.7 and 21°C. (d) pH 5.8, OD 0.7, 21°C. (e) pH 5.2, OD 0.3 and 24°C. (f) pH 5.8, OD 0.3 and 24°C. (g) pH 5.2, OD 0.7 and 24°C. (h) pH 5.8, OD 0.7 and 24°C. (i, j) GUS quantification in GUS-stained percentage of callus growing at pH 5.8. Different letters represent statistical differences. (h) GUS-stained calli with optimum conditions. ($P < 0.05$, Tukey´s HSD test).

Figure 2. Schematic representation of the construct pG3K-WO-AG used in this work and tissue culture progression. (a) Excision-based construct using morphogenic regulators, ABA-inducible *MoCRE* and *nptII* as a selection marker. (b) Isolated immature embryos ranging from 1.3 to 2.15 mm. (c-e) GUS-stained calli at 7, 14 and 21 days after infection. (c) Callus induction in resting medium 7 days after infection. It is noticeable the formation of embryogenic and non-embryogenic tissue (ET and NET) in the immature embryo scutellum. (d) Somatic embryogenesis induction in Maturation I medium 14 days after infection. There is already presence of globular embryos (GE) and scutellar embryos (SE) where *GUS* expression is present. (e) Somatic embryo maturation in Maturation I medium 21 days after infection and just before cassette excision. There is presence of coleoptilar embryos (CE) and the cell clusters expressing *GUS* are bigger. (f-h) Detailed pictures of calli overexpressing the membrane-protein in the GOI cassette 36 and 66 days after infection. (f) Germination of somatic embryos in Maturation II medium 36 days after infection. (g-h) Rooted plantlets in rooting media 66 days after infection.

Figure 3. Flow chart of excision-based Tx430 sorghum transformation protocol.

Figure 4. Phenotypes and confocal imaging pictures of transgenic plants with integrated membrane protein-GFP fusion and non-transgenic plants. Phenotypes observed in sorghum transgenic plants carrying the morphogenic regulator cassette (b), not carrying it (c, d), and escapes (a). (e,f) Yellow channel (GFP) shows the localization of membrane-localized protein and grey channel (bright field) shows the root tissue. (e) GFP absence in non-transgenic root meristem. (f) GFP presence in transgenic root meristem. Images were acquired in FV1000 Olympus confocal microscope.

Figure 5. Transformation of the maize inbred line B104 using pVS1-VIR2 combined with *ZmBbm* and *ZmWUS2*. (a-b) Immature maize embryos transformed with LBA4404 containing pVS1-VIR2 and the binary vector pG3K-ZmUbi$_{pro}$::GUS-intron:tBdUBI1-C (a) and pG3K-WO-ZmUbi$_{pro}$::GUS-intron:tBdUBI1-C (b) were stained for GUS expression 7 days after co-cultivation to visualize transient transformation and formation of somatic emrbyos. Scale bar: 1 mm. (c-d) Representative images of maize plantlets regenerating on maturation medium containing G418 for selection. Embryos of the same cob, transformed with (c) pG3K-ZmUbi$_{pro}$::GUS-intron:tBdUBI-C or (d) pG3K-WO-ZmUbi$_{pro}$::GUS-intron:tBdUBI-C. (e) Representative transgenic plant (953-552-O) generated using pG3K-WO-ZmUbi$_{pro}$::GUS-intron:tBdUBI1-C with image of a cob after self-crossing (inset), illustrating normal fertility.

Figure 6. Distribution of regenerant plants by the number of T-DNA copies and excision efficiency in sorghum and maize. The distribution of regenerant plants, analyzed by digital PCR, is shown according to the number of T-DNA copies. The categories are 0, 1, 2, 3, and 4 or more, with the maximum number of T-DNA copies being 8 in sorghum Tx430 and 5 in maize B104. The figure also shows the distribution of regenerant plants with 1 T-DNA copy, with the presence of the *MoCRE* gene.

(XIII) FIGURES

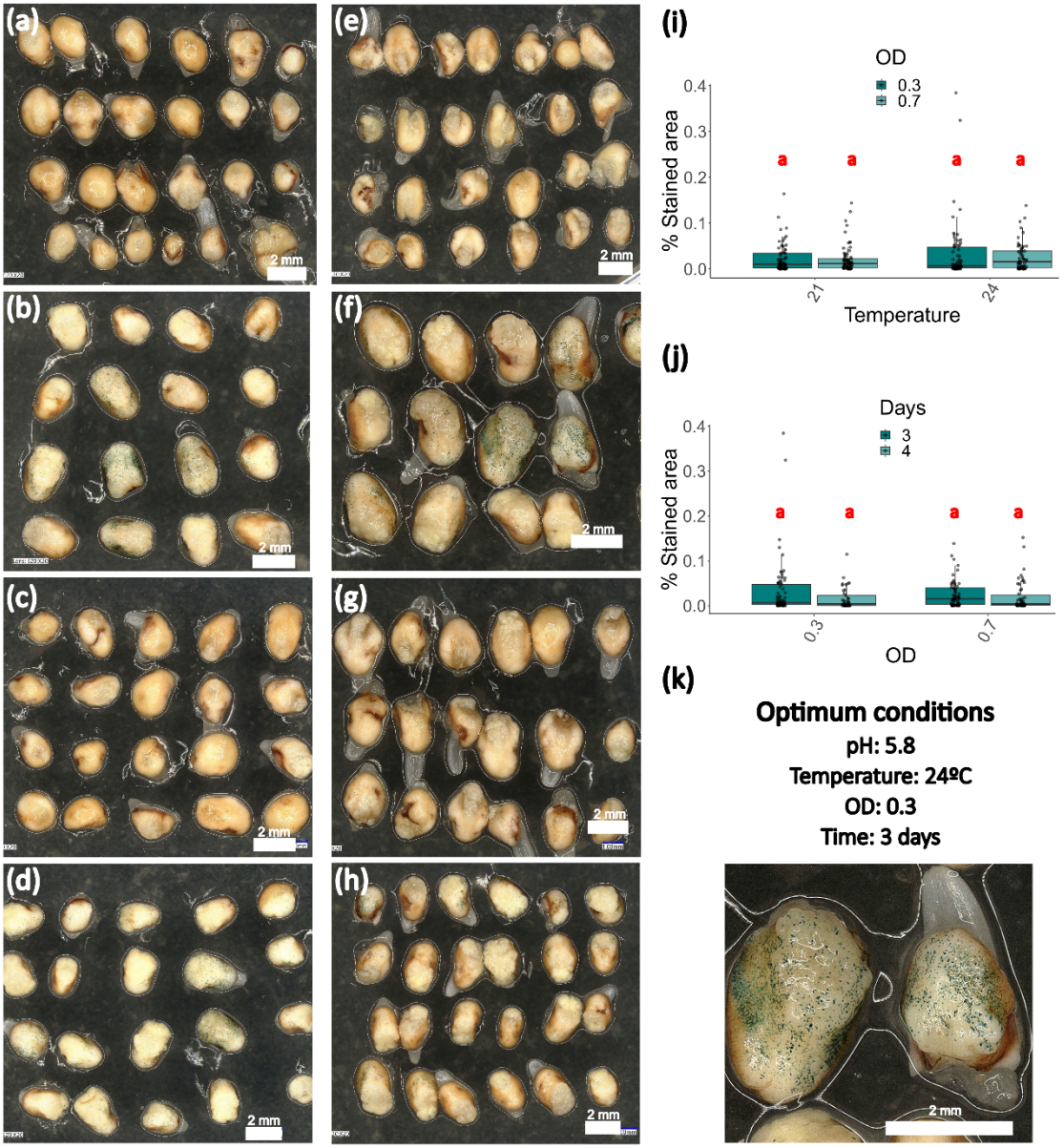

Figure 1. GUS-stained calli and quantification for optimization of infection conditions.

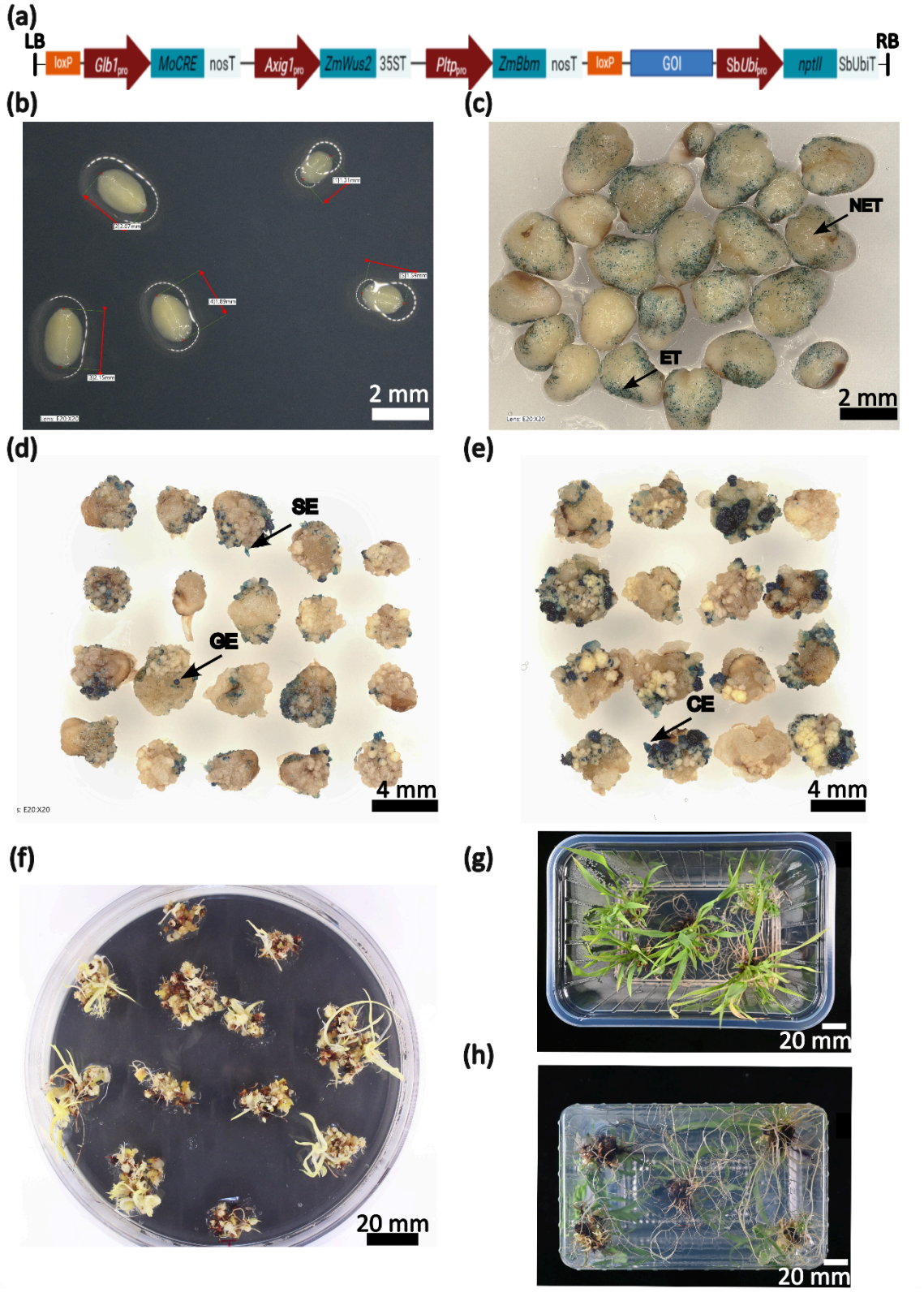

Figure 2. Schematic representation of the construct pG3K-WO-AG used in this work and tissue culture progression.

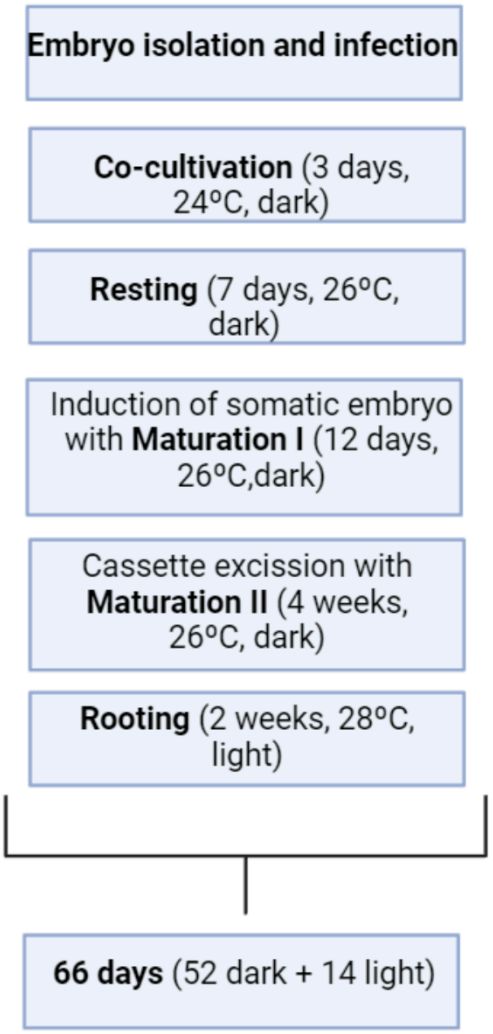

Figure 3. Flow chart of excision-based Tx430 sorghum transformation protocol

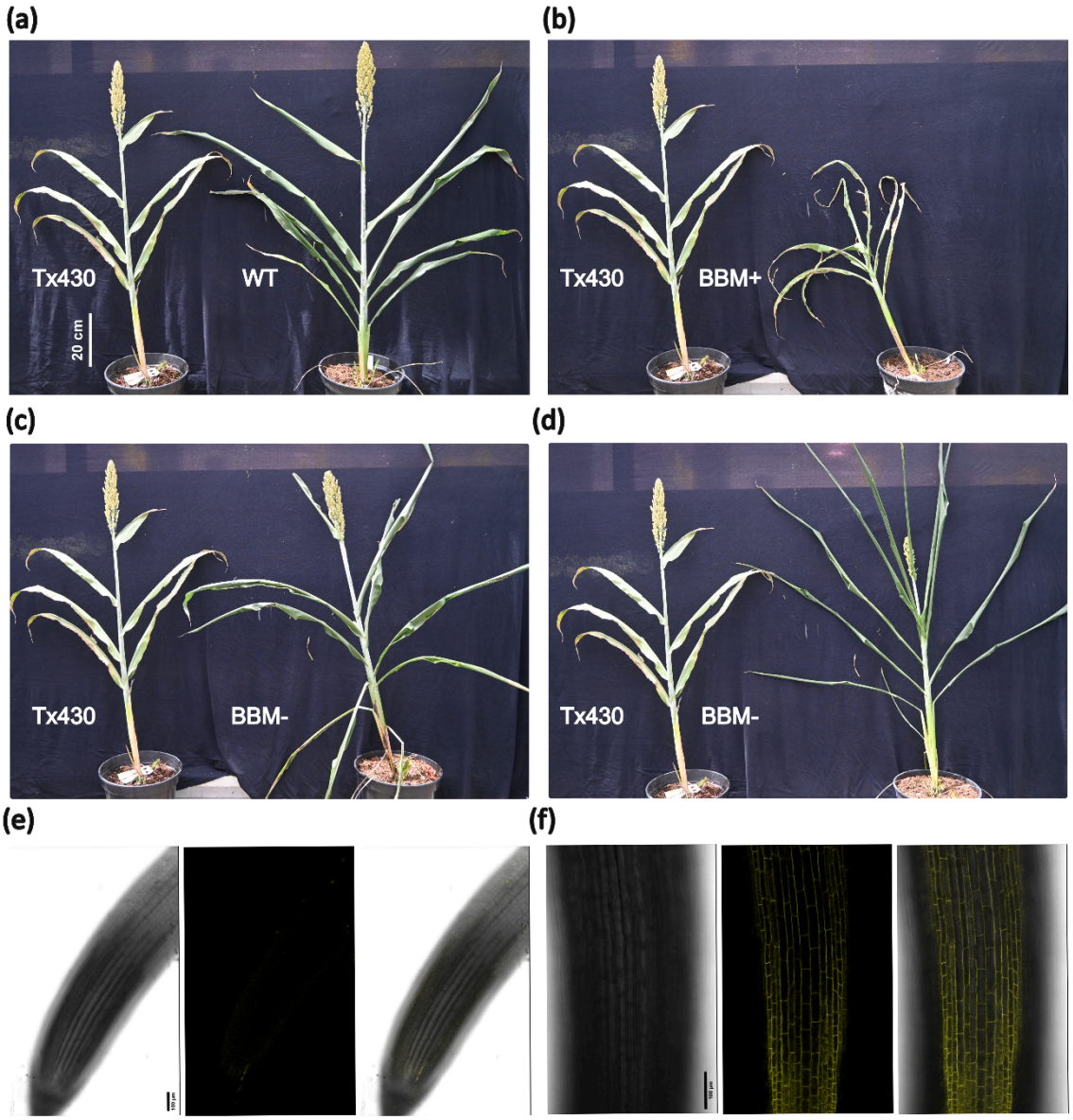

Figure 4. Phenotypes and confocal imaging pictures of transgenic plants with integrated membrane protein-GFP fusion and non-transgenic plants.

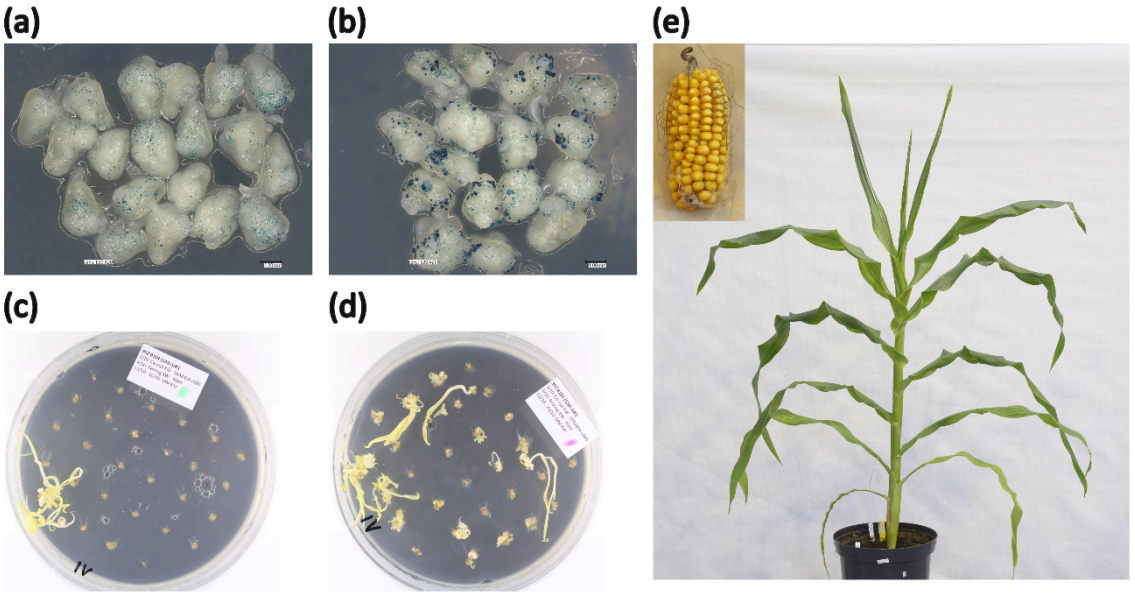

Figure 5. Transformation of the maize inbred line B104 using pVS1-VIR2 combined with *ZmBbm* and *ZmWUS2*.

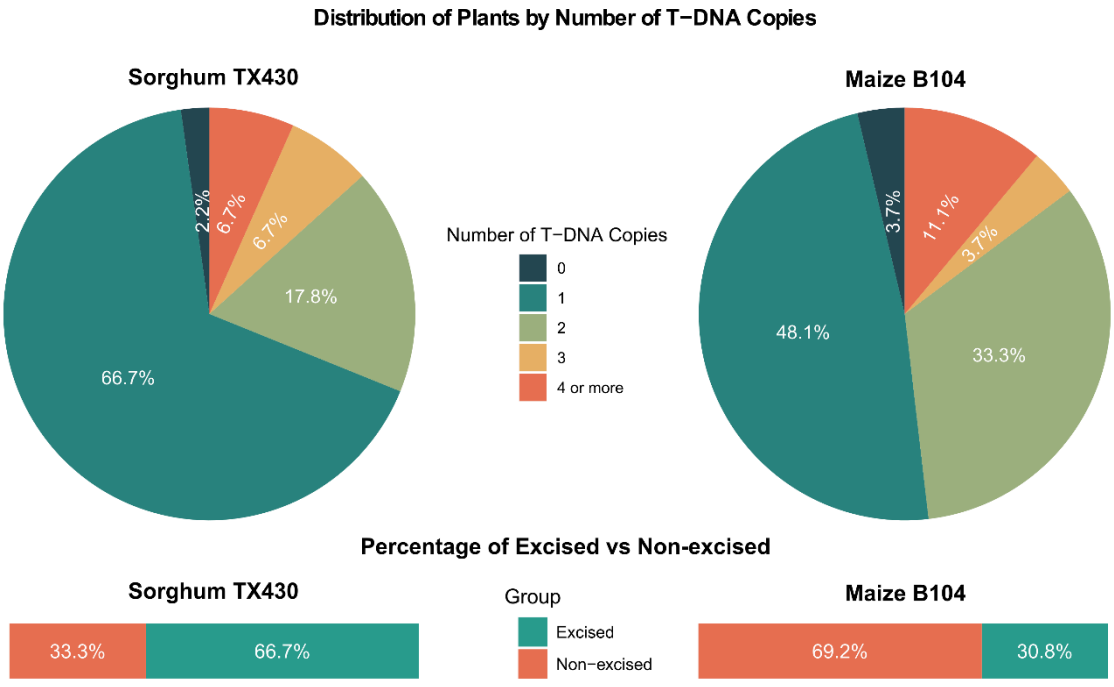

Figure 6. Distribution of regenerant plants by the number of T-DNA copies and excision efficiency in sorghum and maize.

Table 1. Transformation efficiency, escape frequency and excision efficiency in sorghum transformation protocol.

	Starting embryos	Regenerated shoots (Efficiency)[a]	Total isolated plantlets (Efficiency)[b]	Escapes (Frequency)[c]	*MoCRE* absence (Excission efficiency)[d]
Experiment 1	250	77 (30.8%)	415 (166%)	6 (7%)	63 / 93 (67.7%)
Experiment 2	125	29 (23.2%)	203 (162.4%)	0 (0%)	Not available

Table S1. Medium composition for sorghum transformation.

	Units	YP media	Infection media	Co-cultivation	Resting	Maturation I	Maturation II	Rooting
MS Basal Salt with vitamins	g		4.43	4.43	4.43			
MS Basal Salt	g					4.3	4.3	2.15
Yeast extract	g	5						
Peptone	g	10						
NaCl	g	5						
Sucrose	g		68.5	20	20		60	40
Glucose	g		36	10	10			
Myo-inositol	mg					250	100	50
Maltose	g					30		
L-proline	mg			700	700	690	700	
Casein hydrolysate	mg					1000		
Thiamine HCL	mg		1	1	1	1		
Ascorbic acid	mg			10	10			
MES	mg			500	500			
Cefotaxime	mg				100	100	100	
Vancomycine	mg				100	100	100	
Acetosyringone	µM		200	200	200			
CuSO4	mg					1.22	1.25	
IAA	mg						1	
Thidiazuron	mg						0.1	
ABA	mg						0.026	
BAP	mg					0.5		
Zeatin	mg						0.5	
2,4-D	mg		1.5	2	2	2		
MS-vitamins stock	ml						1	1
G418	mg						100 / 250	
Gelrite	g						3	3
Agar	g	12		8	8	8		
pH		6.8	5.2	5.8	5.8	5.8	5.8	5.8

Table S2. Oligonucleotides used in this study.

Genotyping			
Primer ID	**Sequence**	**Aim**	**Amplicon length**
GFP Fw	CAA GCT GAC CCT GAA GTT CAT C	Pressence of transgene	663 bp
BdUBI10terminator Rv	CGA CTA CTT CCA AGG GGC AG	Pressence of transgene	663bp
MoCRE Fw	ACC TCA TGG ACA TGT TCC GC	Pressence of BBM/WUS cassette	1133 bp
MoCRE Rv	TTC CAG GAG GCG AAC CAT TG	Pressence of BBM/WUS cassette	1133 bp
dPCR			
Primer ID	**Sequence**	**Aim**	
CROPGEN1364	TTTCATCGACTGCGGTAGAC	nptII	
CROPGEN1365	AGAAACCTGTCAGCCCATTC	nptII	
CROPGEN1366	CAGGACATCGCCCTGGCAACACGC	nptII probe	
CROPGEN978	ATTGCATACAACACGCTCCT	moCRE	
CROPGEN979	GGTCCTGCCAATGTGGATAA	moCRE	
CROPGEN980	CGCGTGAAGGACATTAGCCGCACCG	moCRe (probe)	
CROPGEN1097	CTTTCAGGGGGTGTTTGGAT	ZmFGPS (reference)	
CROPGEN1098	TGCTCACAGGCAACAAAGTA	ZmFGPS (reference)	
CROPGEN1099	ACCAGGGTCCCAAGCAAACATGCCCA	ZmFGPS probe (reference)	
CROPGEN1361	TGAGGACCCTTTTGATCAGG	SbENOL2 (reference)	
CROPGEN1362	CAAGCCTTCTTGCCAATAGC	SbENOL2 (reference)	
CROPGEN1363	TGGAGTTCATGGGCATCATTGCA	SbENOL2 probe (reference)	
CROPGEN972	AAGTATGGGCATCATTCGCA	GmR (backbone)	
CROPGEN973	ATGTTGGGAGTAGGTGGCTA	GmR (backbone)	
CROPGEN974	GGCTCGGCCCTGACCAAGTCAAATCCA	GmR probe (backbone)	

Table S3. DNA sequences of elements synthesized in this study. *BsaI* restriction sites are indicated in red, GreenGate overhang in green, and start- and stop codons in blue.

BsaI-A-pSbUBI-C-BsaI (1677bp)

ggtctcaacctatgaaactgtgcagccagatgattgacaatcgcaatacttcaactagtgggccatgcacatcagcgacgtgtaacgtcgtgagttgctgttcccgtagagaaaatatcaactggtgggccacgcacatcagcgtcgtgtaacgtggacggaggagcccgtgacggcgtcgacatcgaacggccaccaaccacggaaccacccgtcccccacctctcggaagctccgctccacggcgtcgacatctaacggctaccagcaggcgtacgggttggagtggactccttgcctctttgcgctggcggcttccggaaattgcgtggcggagacgaggcgggctcgtctcacacggcacggaagacgtcacgggttcctttcccccacctctcctcttcccccaccgccataaaatagccgacccccctcgccttttctccccaatctcatctcgtctcgtgttgttcggagcacaccacccgccccaaatcgttcttcccgcaagcctcggcgatccttcacccgcttcaaggtacggcgatcgtcttcctcctctagatcggcgtgatctgcaagtagttgatttggtagatggttaggatctgtgcactgaagaaatcatgttagatccgcgatgtttctgttcgtagatggctgggaggtggaatttttgtgtagatctgatatgttctcctgtttatcttgtcacgctcctgcgatttgtgggggattttaggtcgttgatctgggaatcgtgggggttgcttctaggctgttcgtagatgaggtcgttctcacggtttactggatcattgcctagtagatcagctcgggctttcgtctttgtatatggtgcccatacttgcatctatgatctggttccgtggtgttacctaggtttctgcgcctgatttcgtccgatcgatttgttagccatgtggtaaacgtttggtcatggtctgatttagattagatgcgaataggatgatctcgatctagctcttgggattaatatgcatgtgtcaccaatctgttccgtggttaagatgatgaatctatgcttagttaatgggtgtagatatatatgctgctgttcctcaatgatgccgtagcttttacctgagcagcatggatcgtcctgttacttagggagatgcacatgcttatagatcaagatatgtactgctactgttggaattctttagtataccttgatgatcatccatgctcttgttacttgttttggtatacttggatgatggcatgctgctgcttttgttgatttgagcccatccatatctgcatatgtcacatgattaagatgattacgctgtttctgtatgatgccatagcttttatgtgagcaacatgcatcctcctcggttatatgcattaatagatggaagatatctattgctacaatttgatgattattttgtacatacgatgatcaagcatgctcttcatacttttgttgatatactggataatgaaatgctgctgcacgttcattctatagcactaatgatgtgatgaacacgcacgacctgtttgtggcatctgtttgaatgtgttgttgctgttcactagagactgttttattaacctactgctagatacttacccttctgtctgtttattctttgcagccagaatagcggatccgccggcttgagacc

BsaI-C-nptII-D-BsaI (817bp)

Ggtctcaggctatggtcgaacaggacggccctgcatgcaggatcaccagcggcctgggtcgaaagactcttcggctacgactgggcacaacagaccatcgggtgtagcgacgcagctgttttcaggctgtccgcacagggcagacccgttttgttcgtcaaaacagacctgtctggcgcgctcaacgaactgcaagacgaggccgcaagactgagctggcttgctaccacaggcgttccttgtgctgcagtcctcgacgtcgttactgaggctggaagagactggctgctcctgggtgaagtcccaggacaggaccttttgtccagccatctggccaccagccgaaaaggtcagcatcatggcagacgccatgagaagaggctgcacacactcgaccctgccaacatgccccttcgatcaccaggcaaaacacaggatcgagcgcgcaagaacgcgcatggaggctggtttggtcgaccaagatgacctcgacgaggaacaccaaggactggctcctgctgaactcttcgccagactcaaggcgagaatgccagacggtgacgacctggtcgtcacacacggcgacgcttgtctcccaaacataatggtcgagaacggacgcttcagcggtttcatcgactgcggtagactcggagtcgctgacagatacccaggacatcgccctggcaacacgcgacatcgcagaggaactcggaggcgaatgggctgacaggtttctcgtgctctacggtatcgctgctccagacagccagaggatcgcattctacaggctcctcgacgagttctttttagtcagtgagacc

BsaI-E-tSbUBI-F-BsaI (584bp)

ggtctcactgctctgagctaagctagttcgaacggtacccggggatcctctagtgccgtgggtcgtttaagctgccgctgtacctgtgtcgtctggtgccttctggtgtacctgggaggttgtcgtctatcaagtatctgtggttggtgtcatgagtcagtgagtcccaatactgttcgtgtcctgtgtgccattatacccaaaactgttatgggcaaatcatgaataagcttgatgttcgaacttaaaagtctctgctcaatatggtattatggttgttttgttcgtctcctaatatttgcctgggatcaaatttttattggctggtgttcatttgacctccatgttcttgctaggctccctttttttactctacagccataatatgtttgattgtttggtttgttcttttgttgtacacctggttctgtcgagcttagttttcgacactggcttacagcttaacatgttgctatttttattgggttctgattgctagtttttgctgaatccaaaaaccatgttatttatttaaagcgatccaggttattattatgatggtggctaagtttttttttactatgagacc

Table S4. Plasmids used in this study. *KmR*, kanamycin resistance; *GmR*, gentamycin resistance; sf*GFP*, PglpT-sfGFP-TrrfB visual marker for E. coli.

Name	Features	Source
pG3-U1-AG-U9	Gibson destination vector, GmR	Vandeputte *et al*. subm.
pVS1-VIR2	Ternary helper vector	Zhang et al., 2019
pGGIB-U1-linker-U7	Gibson entry vector, KmR	gatewayvectors.vib.be
pGGIB-U7-A-BsaI-sfGFP-BsaI-G-U8	Gibson entry vector, KmR	gatewayvectors.vib.be
pGGIB-U8-pSbUBI-nptII-tSbUBI-U9	Gibson entry vector, KmR	This work
pGGIB-U1-LoxP-U2	Gibson entry vector, KmR	gatewayvectors.vib.be
pGGIB-U2-pZmGLB1-MoCre-tnos-U3	Gibson entry vector, KmR	Aesaert et al., 2022
pGGIB-U3-pZmAXIG1-ZmWUS2-t35S-U4	Gibson entry vector, KmR	Aesaert et al., 2022
pGGIB-U3-pZmAXIG1-ZmWUS2-t35S-U4	Gibson entry vector, KmR	Aesaert et al., 2022
pGGIB-U4-pZmPLTP-ZmBBM-tnos-U5	Gibson entry vector, KmR	Aesaert et al., 2022
pGGIB-U5-LoxP-U6	Gibson entry vector, KmR	gatewayvectors.vib.be
pGGIB-U6-A-BsaI-sfGFP-BsaI-G-U7	Gibson entry vector, KmR	Aesaert et al., 2022
pGGIB-U7-linker-U	Gibson entry vector, KmR	gatewayvectors.vib.be
pG3K-AG	Destination vector, GmR	This work
pG3K-WO-AG	Destination vector, GmR	This work
pG3K-pZmUBI::GUS-intron:tBdUBI1-C	Expression vector, GmR	This work
pG3K-WO-pZmUBI::GUS-intron:tBdUBI1-C	Expression vector, GmR	This work

Table S5. Molecular characterization of sorghum T0 plants using digital PCR. Copy numbers of the selection marker (*nptII*) and vector backbone (*GmR*) were determined using dPCR. Presence of the *MoCRE* gene was used to examine Cre/lox-mediated excision of the morphogenic genes.

Plant number	nptII	GmR	MoCRE
1	0.00	0.00	0.00
2	1.00	0.00	1.00
3	1.00	0.00	0.00
4	2.00	0.00	2.00
5	2.10	1.10	0.90
6	1.00	0.00	0.00
7	1.00	0.00	0.60
8	3.00	0.00	1.10
9	1.10	0.00	0.00
10	3.00	0.00	1.00
11	1.00	0.00	0.00
12	2.90	0.00	0.00
13	1.10	0.00	1.00
14	1.00	0.00	1.10
15	2.10	0.00	0.00
16	2.00	0.00	1.00
17	1.00	1.00	1.00
18	1.00	1.00	1.00
19	1.00	0.00	0.90
20	8.00	6.00	1.00
21	1.40	0.00	0.00
22	1.50	0.00	0.00
23	1.40	0.00	0.00
24	4.60	0.00	1.40
25	2.60	1.20	0.00
26	2.20	0.00	0.00
27	2.00	0.00	0.00
28	1.00	0.00	0.00
29	1.40	0.00	0.00
30	1.00	0.00	0.00
31	1.00	0.00	0.00
32	2.00	1.10	0.00
33	1.00	1.00	0.00
34	1.00	0.00	0.00
35	3.90	1.40	0.00
36	1.00	0.00	0.00
37	1.00	0.60	0.00
38	1.10	0.30	0.00
39	1.00	0.00	0.00
40	1.00	0.00	0.00
41	0.80	2.00	0.00
42	1.40	0.00	1.30
43	1.00	1.00	0.00
44	0.90	0.40	0.00
45	1.00	0.00	1.00

Table S6. Molecular characterization of maize T0 plants using digital PCR. Copy numbers of the selection marker (*nptII*) and vector backbone (*GmR*) were determined using dPCR. Presence of the *MoCRE* gene was used to examine Cre/lox-mediated excision of the morphogenic genes. When multiple plants were derived from the same immature embryo they are given an additional lowercase letter.

Control			
Plant ID	nptII	GmR	MoCRE
1	0.70	0.00	N/A
2	1.00	0.00	N/A
3	2.30	1.90	N/A
4	0.90	0.00	N/A
5	1.50	0.00	N/A
6	1.60	0.10	N/A
Morphogenic regulators			
Plant ID	nptII	GmR	MoCRE
1	5.40	1.70	6.80
2	1.90	0.00	0.70
3	2.00	0.00	1.20
4	0.80	0.00	0.90
5	1.80	0.00	1.20
6	0.80	1.10	0.00
7	0.80	0.00	0.80
8	1.10	1.00	0.00
9	2.20	0.00	2.20
10	2.00	0.00	1.00
11	4.70	0.00	2.00
12	2.10	0.00	3.10
13	1.10	0.00	1.00
14	1.40	1.20	0.80
15	1.10	0.00	1.30
16	1.00	0.00	1.00
17	1.20	0.00	0.20
18	2.50	0.00	0.00
19	1.10	0.00	1.10
20	4.90	0.00	5.00
21	0.80	0.00	1.00
22	0.90	0.00	0.80
23	2.90	0.70	4.10
24	0.00	0.00	0.00
25	2.00	0.60	1.10
26	0.90	0.00	1.30
27	2.10	0.00	0.90

Figure S1: Immature sorghum embryo isolation procedure. (a) Position the seed with tweezers, ensuring the embryo side (opposite the hilum) is facing upward. (b) Use a lancet to create a small aperture at the tip of the seed. (c) Gently press the lancet at the bottom of the seed, taking care to avoid damaging the embryo. (d) Extract the embryo with the tip of the lancet and transfer it into microcentrifuge tubes.

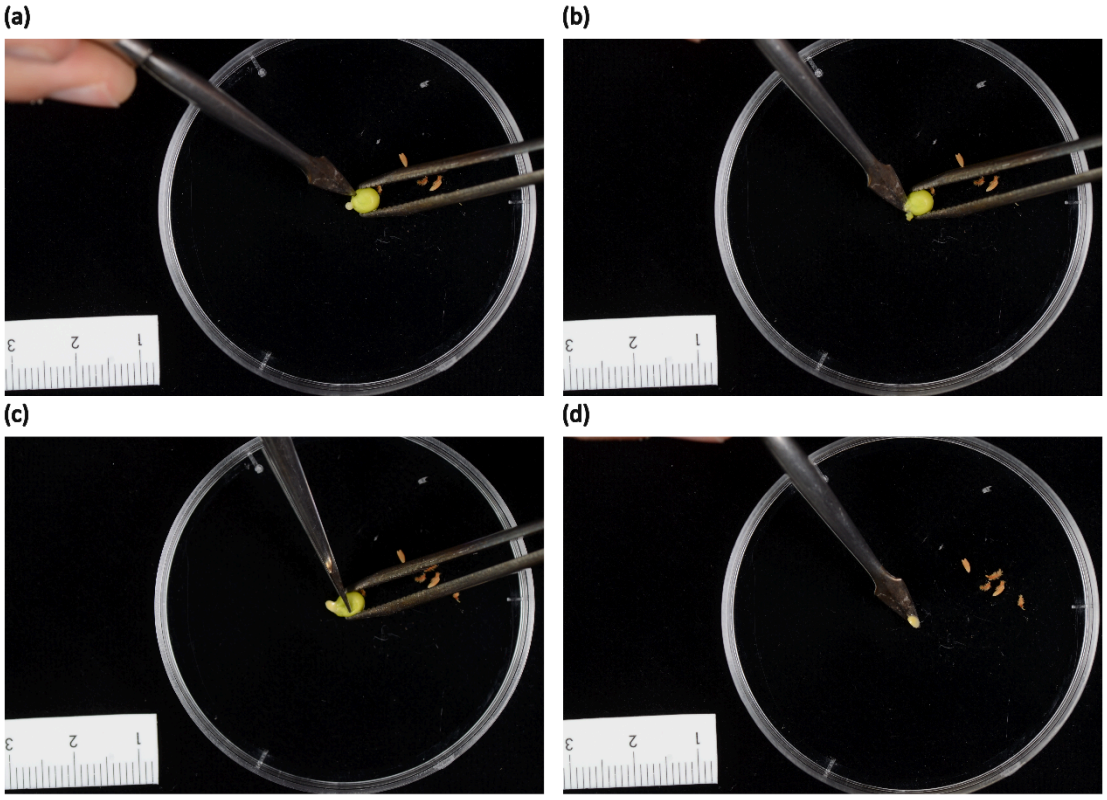

Figure S2. Gel electrophoresis of amplified DNA by PCR in transgenic and non-transgenic (WT) plants. Plasmid DNA was also amplified as a positive control. The amplicon length is 663 bp for the GOI region and 1133 bp for the excision cassette region.